SUPERNOVA REMNANTS II
AN ODYSSEY IN SPACE AFTER STELLAR DEATH
3-8 JUNE 2019, CHANIA, CRETE, GREECE

Nucleosynthesis Constraints on The Energy Growth Timescale of a Core-Collapse Supernova Explosion

Ryo Sawada[1] **and Keiichi Maeda**[1]

[1] Department of astronomy, Kyoto University, Kitashirakawa-Oiwake-cho, Sakyo-ku, Kyoto 606-8502, Japan

Abstract

Details of the explosion mechanism of core-collapse supernovae (CCSNe) are not yet fully understood. There is an increasing number of numerical examples by ab-initio core-collapse simulations leading to an explosion. Most, if not all, of the ab-initio core-collapse simulations represent a 'slow' explosion in which the observed explosion energy ($\sim 10^{51}$ ergs) is reached in a timescale of $\gtrsim 1$ second. It is, however, unclear whether such a slow explosion is consistent with observations. In this work, by performing nuclear reaction network calculations for a range of the explosion timescale $t_{\rm grow}$, from the rapid to slow models, we aim at providing nucleosynthetic diagnostics on the explosion timescale. We employ one-dimensional hydrodynamic and nucleosynthesis simulations above the proto-neutron star core, by parameterizing the nature of the explosion mechanism by $t_{\rm grow}$. The results are then compared to various observational constraints; the masses of ^{56}Ni derived for typical CCSNe, the masses of ^{57}Ni and ^{44}Ti observed for SN 1987A, and the abundance patterns observed in extremely metal-poor stars. We find that these observational constraints are consistent with the 'rapid' explosion ($t_{\rm grow} \lesssim 250$ ms), and especially the best match is found for a nearly instantaneous explosion ($t_{\rm grow} \lesssim 50$ ms). Our finding places a strong constraint on the explosion mechanism; the slow mechanism ($t_{\rm grow} \gtrsim 1000$ ms) would not satisfy these constraints, and the ab-inito simulations will need to realize a rapid explosion.

1 Introduction

Core-collapse supernovae (CCSNe) occur at the end of the lives of massive stars ($M_{\rm ZAMS} > 8M_\odot$) (Baade & Zwicky, 1934). However, the detailed nature of the explosion mechanism remains unclear. The most promising scenario is the delayed neutrino-driven explosion (Bethe & Wilson, 1985). There is an increasing number of numerical examples by ab-initio core-collapse simulations leading to an explosion (see e.g., Janka 2012 and references therein).

Most, if not all, of the ab-initio core-collapse simulations represent a 'slow' explosion in which the observed explosion energy ($\sim 10^{51}$ ergs) is reached in a timescale of $\gtrsim 1$ second. However, it is unclear whether the nature of the explosion shown by these simulations is consistent with observations.

In this work, by performing the nuclear reaction network calculation for a range of the explosion timescale, from the rapid to slow models, we aim at providing nucleosynthetic diagnostics on the explosion timescale ($t_{\rm grow}$; the timescale in which the explosion energy is reached to 10^{51} ergs since the initiation of the explosion). In doing this, we compare our results to various observational constraints; the masses of ^{56}Ni derived for typical CCSNe, the masses of ^{57}Ni and ^{44}Ti observed for SN 1987A, and the abundance patterns observed in the extremely metal-poor (EMP) stars. By these comparisons, we discuss the appropriate energy growth timescale for typical CCSN explosion mechanism, i.e., an important constraint on the nature of the explosion.

2 Models

Our simulation is opted to remove the proto-neutron star (PNS) core and drive an explosion by injecting constant energy at the PNS surface. The energy input is terminated when a desired explosion energy ($E_{\rm exp}$) is reached. The constant energy input rate is thus modeled as follows:

$$\dot{E}_{\rm exp} = E_{\rm exp}/t_{\rm exp} = (E_{\rm final} + |E_{\rm bind}|)/t_{\rm exp} \ , \tag{1}$$

$$t_{\rm exp} = \frac{E_{\rm exp}}{E_{\rm ref} + |E_{\rm bind}|} \times t_{\rm grow} \ , \tag{2}$$

where $E_{\rm final}$ is the final energy of the supernova, and $E_{\rm exp}$ is the total injected energy. $t_{\rm grow}$ is defined as the energy growth timescale in which the explosion energy (i.e., the injected energy subtracted by the bound energy) is reached to the canonical energy ($E_{\rm ref} \equiv 10^{51}$ ergs) of the explosion in normal CCSNe. In this study, we treat $t_{\rm grow}$ and $E_{\rm final}$ as free parameters which reflect the nature of the explosion mechanism (Figure 1).

3 Numerical Method

We solve the 1D Newtonian hydrodynamics with the Helmholtz equation of state (Timmes & Swesty, 2000) by using `blcode`[1] (Morozova et al., 2015) . Our calculation includes a nuclear burning to follow the energy generation, by solving a 21 α-isotope reaction network [2](Weaver et al., 1978). For a more accurate assessment of the nucleosythesis, a post-processing analysis is performed with a nuclear reaction network including 640-nuclear species (Timmes, 1999).

The pre-explosion structures are solar-metallicity, non-rotating stellar models obtained by the stellar evolution code `MESA` (Paxton et al., 2015). We adopt the 3 pre-explosion models with $M_{\rm ZAMS}$ =15.0, 20.0, and 25.0 $M_\odot$.

[1]https://stellarcollapse.org/SNEC
[2]http://cococubed.asu.edu/code_pages/codes.shtml

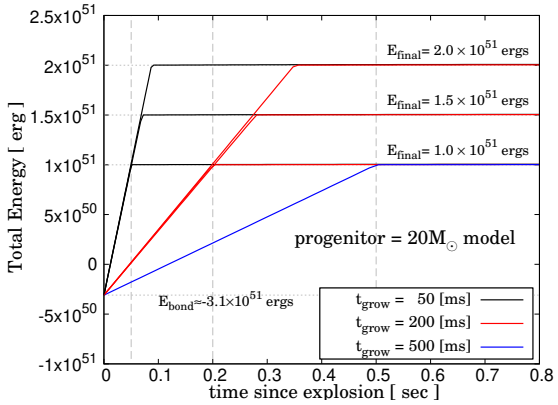

Figure 1: The relation between the definition of $t_{\rm grow}$ and the final energy $E_{\rm final}$. The line color corresponds to each $t_{\rm grow}$.

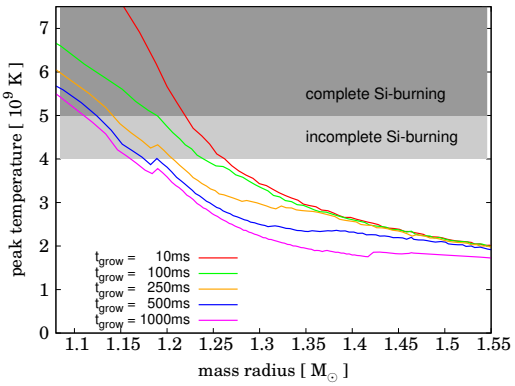

Figure 2: The peak temperature evolution behind the shock wave as a function of the enclosed mass M_r, for the energy growth timescale $t_{\rm grow}$=10, 100, 250, 500, 1000 msec, for the model with $M_{\rm ZAMS} = 20M_\odot$ and $E_{\rm final} = 1.0 \times 10^{51}$ ergs.

4 Results: Temperature profiles

Figure 2 shows the temperature evolution just behind the shock wave. There is a clear difference in the mass coordinate that the shock wave sweeps until the temperature decreases below $T \sim 5 \times 10^9$ K (shown by the dark gray region). In the instantaneous explosion model ($t_{\rm grow}$=10 ms), a strong shock propagates up to $M_r \approx 1.22M_\odot$ keeping a $T > 5 \times 10^9$ K to trigger the Si-burning. On the other hand, in the slow explosion model (e.g., $t_{\rm grow}$=1000 ms), the shock is weak, and the temperature decreases to $T < 5 \times 10^9$ K before a shock reaches to $M_r \approx 1.10M_\odot$. That is, it is estimated that the complete Si-burning product in the slow explosion model would be about $\sim 0.1M_\odot$ less than that in the instantaneous explosion model.

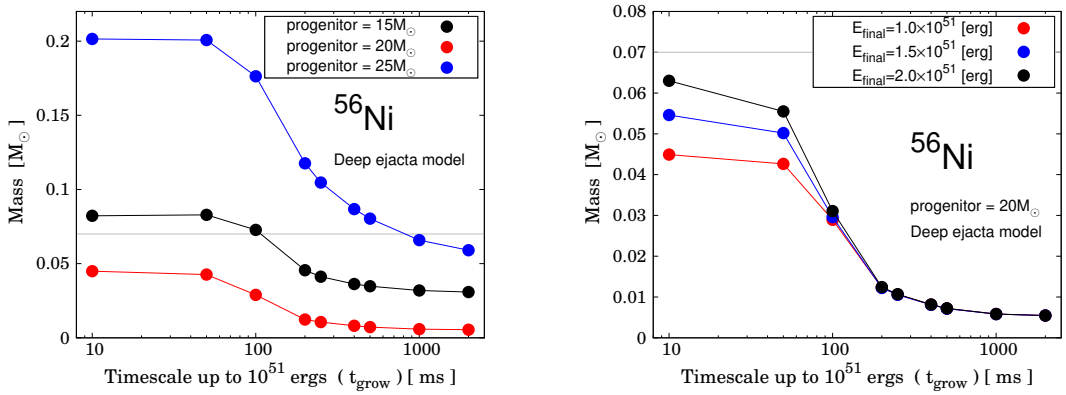

Figure 3: The energy growth timescale $t_{\rm grow}$ and the produced ^{56}Ni mass; with the 3 progenitor mass and $E_{\rm final} = 1.0 \times 10^{51}$ models, and with the 3 different final/total energy $E_{\rm final}$ and $20M_\odot$ models. The gray line corresponds to $M(^{56}{\rm Ni}) = 0.07M_\odot$.

5 Comparison to Observations

5.1 ^{56}Ni produced in typical CCSNe

The amount of ^{56}Ni ejected in individual SNe, which drives supernova brightness, is an important diagnosing indicator of the supernova explosion. It is estimated that, in 'typical supernovae', on average $\sim 0.07M_\odot$ of ^{56}Ni should be synthesized (e.g., Hamuy 2003).

Figure 3 shows the relation between the energy growth timescale $t_{\rm grow}$ and the synthesized ^{56}Ni mass. It can be clearly seen that there is a decreasing tendency of $M(^{56}{\rm Ni})$ for increasing $t_{\rm grow}$. This decreasing trend of $M(^{56}{\rm Ni})$ comes from the suppression of the peak temperature as increasing $t_{\rm grow}$, as can be seen in Fig.2. The amount of synthesized ^{56}Ni serves as a strong constraint on the CCSN explosion mechanism (which confirms the suggestion by Suwa et al. 2019); the argument related to $M(^{56}{\rm Ni})$ strongly supports the rapid explosion ($t_{\rm grow} < 500$ msec), and the models with $t_{\rm grow} \gtrsim 1000$ msec would never explain the nature of typical CCSNe.

5.2 ^{44}Ti and ^{57}Ni produced in SN1987A

Figures 4 shows the relation between $t_{\rm grow}$ and the synthesized ^{57}Ni and ^{44}Ti masses. In view of the observational properties of SN1987A, we have found that the instantaneous explosion model ($t_{\rm grow} \lesssim 100$ msec) can roughly satisfy these constraints, while the increase of $t_{\rm grow}$ tends to suppress the synthesized amounts of these isotopes. Note that this simulation is not tuned to mimic SN1987A and multi-dimensional effects in the explosion may also be a key in the synthesis of ^{44}Ti (Nagataki et al. 1998; Maeda & Nomoto 2003). However, we find that combined analysis of ^{56}Ni, ^{57}Ni, and ^{44}Ti strongly disfavors the slow explosion model with $t_{\rm grow} \gtrsim 1000$ msec as the CCSNe explosion mechanism.

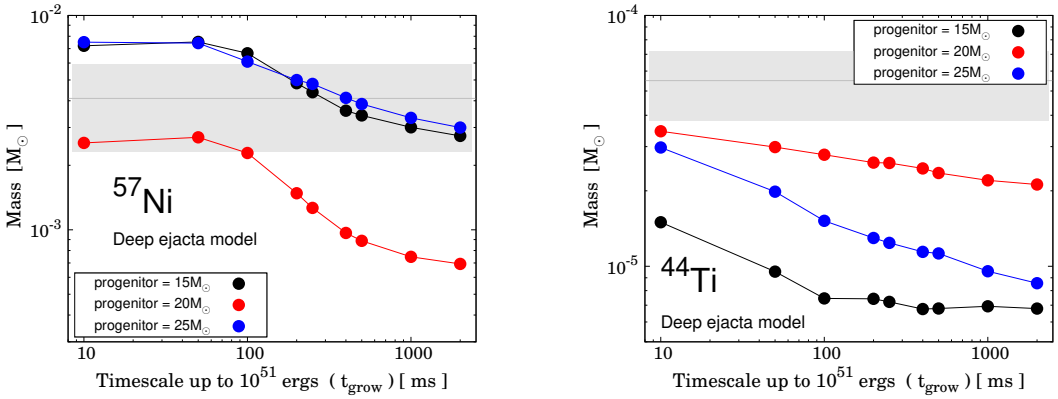

Figure 4: The energy growth timescale $t_{\rm grow}$ and the produced ^{57}Ni and ^{44}Ti mass. Show here is dependence on $M_{\rm ZAMS}$ (for given $E_{\rm final} = 1.0 \times 10^{51}$). The gray region shows to $M(^{57}{\rm Ni}) = 0.0041 \pm 0.0018 M_\odot$, and $M(^{44}{\rm Ti}) = 0.55 \pm 0.17 \times 10^{-4} M_\odot$ (Seitenzahl et al., 2014).

5.3 Comparison to the abundances of extremely metal-poor stars

As described in Tominaga et al. 2007 and Heger & Woosley 2010, it can be assumed that the EMP stars preserve individual CCSN abundance patterns. Therefore, we follow this strategy, by requiring that the typical CCSN yields should be consistent with the abundance patterns of EMP stars, and consider to constrain the explosion mechanism of 'typical supernovae'.

The relation between $t_{\rm grow}$ and [Mn/Fe] and [Co/Fe] is shown in Figure 5. There is the increasing trend of [Mn/Fe] and the decreasing trend of [Co/Fe] for increasing $t_{\rm grow}$, resulting in a substantial discrepancy between the observations and the slow explosion models ($t_{\rm grow} \gtrsim 1000$ ms). These elements, Mn and Co, are dominated by the decay products of ^{55}Co and ^{59}Cu, respectively. Regarding the ambiguity in Ye (implicitly the metallicity of the progenitor), both of ^{55}Co and ^{59}Cu are neutron-rich isotopes, so both of [Mn/Fe] and [Co/Fe] tend to be smaller for larger Ye. Therefore,these opposite trends strongly support the rapid explosion model ($t_{\rm grow} \lesssim 250$ ms). In summary, we conclude that Mn/Fe and Co/Fe are important indicators which reflect the nature of the explosion regardless of the natures of the progenitor stars (i.e., mass $M_{\rm ZAMS}$ and metallicity $Z_{\rm ZAMS}$).

Acknowledgments

The authors thank Yudai Suwa for stimulating discussion, and Ryoma Ouchi for kindly providing the progenitor model. The work has been supported by Japan Society for the Promotion of Science (JSPS) KAKENHI Grant 17H02864, 18H04585, 18H05223 (K.M.) and 19J14179 (R.S.).

References

Baade, W., & Zwicky, F. 1934, Proceedings of the National Academy of Science, 20, 254

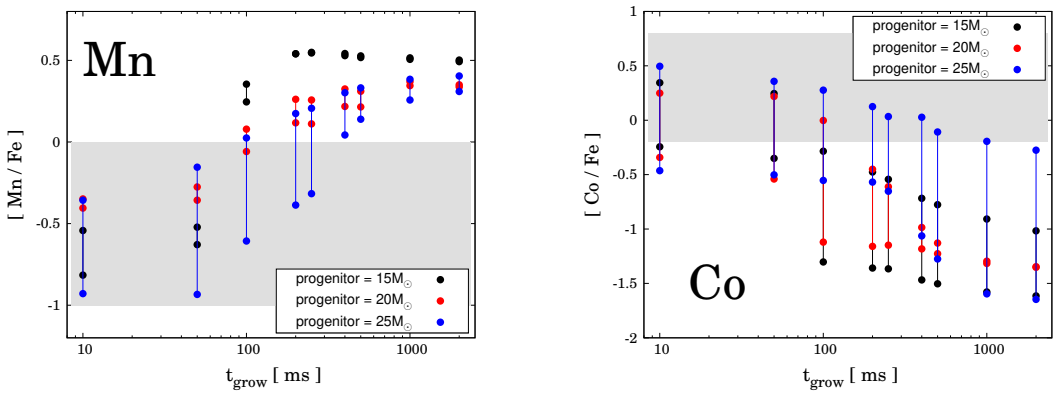

Figure 5: The relation between the energy growth timescale with [Mn/Fe] and [Co/Fe]. The left panel shows the models with $M_{\rm ZAMS} = 15,\ 20,\ 25\ M_\odot$, all of which have $E_{\rm final} = 1.0 \times 10^{51}$ erg. The gray region corresponds to $-1.0 <$[Mn/Fe]< 0.0 and $-0.2 <$[Co/Fe]< 0.8 (McWilliam et al. 1995; Ryan et al. 1996; Cayrel et al. 2004; Honda et al. 2004).

Bethe, H. A., & Wilson, J. R. 1985, ApJ, 295, 14

Cayrel, R., et al. 2004, A&A, 416, 1117

Hamuy, M. 2003, ApJ, 582, 905

Heger, A., & Woosley, S. E. 2010, ApJ, 724, 341

Honda, S., Aoki, W., Kajino, T., Ando, H., Beers, T. C., Izumiura, H., Sadakane, K., & Takada-Hidai, M. 2004, ApJ, 607, 474

Janka, H.-T. 2012, Annual Review of Nuclear and Particle Science, 62, 407

Maeda, K., & Nomoto, K. 2003, ApJ, 598, 1163

McWilliam, A., Preston, G. W., Sneden, C., & Searle, L. 1995, AJ, 109, 2757

Morozova, V., Piro, A. L., Renzo, M., Ott, C. D., Clausen, D., Couch, S. M., Ellis, J., & Roberts, L. F. 2015, ApJ, 814, 63

Nagataki, S., Hashimoto, M.-a., Sato, K., Yamada, S., & Mochizuki, Y. S. 1998, ApJl, 492, L45

Paxton, B., et al. 2015, ApJs, 220, 15

Ryan, S. G., Norris, J. E., & Beers, T. C. 1996, ApJ, 471, 254

Seitenzahl, I. R., Timmes, F. X., & Magkotsios, G. 2014, ApJ, 792, 10

Suwa, Y., Tominaga, N., & Maeda, K. 2019, MNRAS, 483, 3607

Timmes, F. X. 1999, ApJs, 124, 241

Timmes, F. X., & Swesty, F. D. 2000, ApJs, 126, 501

Tominaga, N., Umeda, H., & Nomoto, K. 2007, ApJ, 660, 516

Weaver, T. A., Zimmerman, G. B., & Woosley, S. E. 1978, ApJ, 225, 1021